Title: Granzyme B prevents aberrant IL-17 production and intestinal pathogenicity in CD4$^+$ T cells

Authors: Kristen L. Hoek, PhD [a]; Michael J. Greer, PhD [b*]; Kathleen G. McClanahan,[a*] Ali Nazmi [a], PhD; M. Blanca Piazuelo, MD[c,e]; Kshipra Singh, PhD[c,e]; Keith T. Wilson, MD[a,c,e,f,g]; and Danyvid Olivares-Villagómez, PhD[a,e,g,h].

*These two authors contributed equally to this report

Affiliations: [a]Department of Pathology, Microbiology and Immunology, Vanderbilt University Medical Center, A5301 Medical Center North, Nashville, Tennessee 37232, USA; [b]Department of Biomedical Informatics, Vanderbilt University, Nashville, Tennessee, 37232, USA; [c]Division of Gastroenterology, Hepatology and Nutrition, Department of Medicine, Vanderbilt University Medical Center, Nashville, Tennessee 37232, USA; [e]Center for Mucosal Inflammation and Cancer, Vanderbilt University Medical Center, Nashville, Tennessee 37232; [f]Veterans Affairs Tennessee Valley Healthcare System, Nashville, Tennessee 37232; [g]Vanderbilt Institute for Infection, Immunology and Inflammation, Vanderbilt University Medical Center, A5301 Medical Center North, Nashville, Tennessee 37232, USA. [h]ORCID, 0000-0002-1158-8976

Corresponding author: Danyvid Olivares-Villagómez. Address: Vanderbilt University Medical center, A5211 Medical Center North, Nashville Tennessee 37232-0001. Fax number: 615-343-7392. Telephone number: 615-936-0134. email: danyvid.olivares-villagomez@vumc.org.

Conflict of Interest: No conflict

Author contributions: K.L.H., and D.O-V. designed research; K.L.H., M.J.G., K.M., A.N., and K.S. performed research; K.L.H., M.J.G., M.B.P. and D.O-V. analyzed data; K.S. and K.T.W. provided expertise with *Citrobacter rodentium* infections; K.L.H. and D.O-V. wrote the manuscript.

Acknowledgments

This work was supported by NIH grant R01DK111671 (D.O-V.); National Library of Medicine T15 LM00745 (M.J.G.); Vanderbilt Training in Cellular, Biochemical and Molecular Sciences Training Program, T32 GM008554-25 (K.G.M.); Vanderbilt Training in Gastroenterology T32 grant NIH T32 DK007673 (A.N.); and the Digestive Disease Research Center at Vanderbilt University Medical Center, NIH grant P30DK058404 (M.B.P., K.T.W., and D.O-V.). Flow cytometry experiments were performed in the VMC Flow Cytometry Shared Resource, supported by the Vanderbilt Ingram cancer Center (P30 CA068485) and the Vanderbilt Digestive Disease Research Center (DK058404). We acknowledge the Translational Pathology Shared Resource supported by NCI/NIH cancer Center Support Grant 5P30 CA68485-19 and the Mouse Metabolic Phenotyping Center Grant 2 U24 DK059637-16. We also thank the Vanderbilt Technologies for Advanced Genomics (VANTAGE) for their invaluable support.

Key words: Granzyme B; $CD4^+$ T cells; T cell differentiation; IL-17; intestinal inflammation.

Abstract: $CD4^+$ T cell activation and differentiation are important events that set the stage for proper immune responses. Many factors are involved in the activation and differentiation of T cells, and these events are tightly controlled to prevent unwanted and/or exacerbated immune responses that may harm the host. It has been well documented that granzyme B, a potent serine protease involved in cell-mediated cytotoxicity, is readily expressed by certain $CD4^+$ T cells, such as regulatory T cells and $CD4^+CD8\alpha\alpha^+$ intestinal intraepithelial lymphocytes, both of which display cytotoxicity associated with granzyme B. However, because not all $CD4^+$ T cells expressing granzyme B are cytotoxic, additional roles for this protease in $CD4^+$ T cell biology remain unknown. Here, using a combination of *in vivo* and *in vitro* approaches, we report that granzyme B-deficient $CD4^+$ T cells display increased IL-17 production. In the adoptive transfer model of intestinal inflammation, granzyme B-deficient $CD4^+$ T cells triggered a more rapid disease onset than their WT counterparts, and presented a differential transcription profile. Similar results were also observed in granzyme B-deficient mice infected with *Citrobacter rodentium*. Our results suggest that granzyme B modulates $CD4^+$ T cell differentiation, providing a new perspective into the biology of this enzyme.

Introduction

Granzymes are a family of serine proteases expressed by many immune cell populations. There are five different granzymes in humans (A, B, H, K and M) and 11 in mice (A, B, C, D, E, F, G, K, L, M and N), which differ in function and substrate specificity.[1] Most research has focused on granzymes A and B due to their hallmark role in $CD8^+$ T and NK cell-mediated cytotoxicity against tumor cells or virus-infected cells.[2] However, mounting evidence indicates that granzymes are also involved in other processes, including inflammatory responses,[3-5] remodeling of the extracellular matrix,[6] and cardiovascular disorders.[7]

Activated $CD4^+$ T cells express granzyme B, and some of these cells exhibit lytic activity similar to $CD8^+$ T cells.[8, 9] Antigen-specific $CD4^+$ T cell lytic activity mediated by granzyme B can be triggered by viral and bacterial infections.[10-12] Similarly, some tumor-infiltrating $CD4^+$ T cells also present anti-tumor cytotoxicity mediated by granzyme B.[13] In addition, one of the mechanisms by which regulatory $CD4^+$ T cells in humans and mice control immune responses is through granzyme B-mediated cell death.[14-18]

After activation, $CD4^+$ T cells can differentiate into a diverse set of T helper (Th) cells depending on environmental cues and transcription factors, which ultimately leads Th cells to produce a specific cytokine profile.[19] In certain populations of differentiated $CD4^+$ T cells, granzyme B controls $CD4^+$ T cell immune responses by initiating activation-induced cell death.[20] Downregulation of granzyme B, for example when Th2 cells are cultured in the presence of vasoactive intestinal peptide, reduces Th2 cell death.[20] Moreover, granzyme B expression in Th2 cells is enhanced by IL-10R signaling, which results in cell death.[21] These studies clearly indicate that granzyme B is involved in controlling some immune $CD4^+$ T cell responses. However, it is unclear whether this enzyme is actively involved during the process of Th differentiation.

In this report, we present data indicating that granzyme B is expressed during $CD4^+$ T cell differentiation. Cells lacking granzyme B show a different cytokine profile than granzyme B-competent cells, primarily presenting increased IL-17 production. Moreover, using the adoptive transfer model of intestinal inflammation, we show that granzyme B-deficient $CD4^+$ T cells activated *in vivo* have a different gene expression profile and display increased pathogenicity relative to WT cells. Similarly, we present evidence indicating that granzyme B deficiency predisposes mice to higher susceptibility to *Citrobacter rodentium* infection. These results indicate that granzyme B is required for proper $CD4^+$ T cell differentiation, and in its absence, $CD4^+$ T cells may acquire an aberrant phenotype characterized by increased IL-17 production and pathogenicity.

Results

Th0 and Th1, but not Th17 $CD4^+$ T cells express granzyme B during differentiation

To determine the role of granzyme B in T cell activation and differentiation, we cultured naïve $CD4^+$ T cells in Th0, Th1 and Th17 differentiation conditions. One and three days after culture, RNA was extracted to determine granzyme B expression relative to naïve $CD4^+$ T cells. Under Th0 conditions, expression of granzyme B at day 1 displayed a slight increase above the levels observed for naïve $CD4^+$ T cells (Figure 1a, top), but presented an almost three-fold increase at day 3 (Figure 1a, bottom). Th1 cells expressed a 3-fold increase in granzyme B mRNA over naïve T cells at day 1, which was maintained until day 3. On the other hand, $CD4^+$ T cells under Th17 differentiation conditions did not induce granzyme B mRNA expression at either time point (Figure 1a).

Around 13% of Th0 and Th1 cells expressed granzyme B intracellularly at day 5 (Figure 1b; see Supplemental Figure 1a for gating strategy), whereas this enzyme was not detected in Th17

cells, confirming the results for granzyme B mRNA expression. Although granzyme B mRNA was detected at day 1 in Th1 cells, granzyme B protein was not, but the protein was conspicuously expressed at day 3 and day 5 (Figure 1c). These results suggest a lag between granzyme B mRNA transcription and translation. A similar granzyme B protein expression profile was detected for Th0 cells (Figure 1c). On the other hand, Th17 cells did not express granzyme B at any of the time points analyzed (Figure 1c). Similarly, Th2 cells did not express granzyme B (Supplemental Figure 2b).

Because Th1 and Th17 cultures contain different cytokine/antibody cocktails, and granzyme B is expressed in the former, but not in the latter, we investigated what factors present in these culture conditions induce or repress granzyme B expression. For this purpose, we activated $CD4^+$ T cells under Th0 conditions (anti-CD3/CD28, IL-2, and irradiated spleen cells), in the presence of individual factors included in Th1 and Th17 differentiation cocktails (Figure 1d). IL-2 alone induced ~7.5% of $CD4^+$ T cells to express granzyme B, which was not significantly different from cells activated without IL-2 (background levels), or in the presence of IL-12, IL-1β, and IL-23, the last two of which are involved in Th17 differentiation. However, the Th17-inducing cytokines IL-6 and TGFβ, as well as the blocking anti-IFNγ antibody, significantly ablated granzyme B expression. These results indicate that $CD4^+$ T cell activation induces granzyme B activation, whereas some cytokines and anti-IFNγ inhibit its expression.

Because most of our differentiation cultures included spleen cells as a source of APC, we determined whether these cells influence granzyme B expression during $CD4^+$ T cell activation. As shown in Figure 1e, $CD4^+$ T cell activation in the absence of APC (but including IL-2), resulted in less than 2% of $CD4^+$ T cells expressing granzyme B, whereas irradiated spleen APC significantly increased granzyme B expression.

Overall, these results indicate that granzyme B is expressed during Th0 and Th1 differentiation, with irradiated APC being an important expression-enhancing factor. On the other hand, Th17 and Th2 differentiation conditions ablate granzyme B expression. This effect can be attributed to IL-6, TGFβ, and anti-IFNγ.

As shown in Figure 1b, during Th0 and Th1 differentiation, two populations of $CD4^+$ T cells can be distinguished: WT-$gzmB^{pos}$ and WT-$gzmB^{neg}$. To determine whether these populations present different cytokine profiles, we determined the frequencies of IFNγ- and IL-17-producing cells in each of these subpopulations. Around half of Th0 WT-$gzmB^{pos}$ expressed IFNγ, whereas only around 5% of the WT-$gzmB^{neg}$ $CD4^+$ T cells were positive for IFNγ (Figure 1f). Th0 cells derived from granzyme B-deficient (*Gzmb*$^{-/-}$) mice presented decreased levels of IFNγ-producing cells in comparison to WT-$gzmB^{pos}$ cells, but significantly more $IFN\gamma^+$ cells than WT-$gzmB^{neg}$ cells (Figure 1f). On the other hand, IL-17 production was not significantly different among Th0 cells from any of the $CD4^+$ T cell populations.

Th1 differentiation induced high levels of $IFN\gamma^+$ cells in all $CD4^+$ T cell populations analyzed; however, WT-$gzmB^{pos}$ cells presented the highest levels of $IFN\gamma^+$ cells in comparison to WT-$gzmB^{neg}$ or cells derived from *Gzmb*$^{-/-}$ mice (Figure 1g). Interestingly, under Th1 conditions, cells from *Gzmb*$^{-/-}$ mice presented significantly greater levels of $IL\text{-}17^+$ cells when compared to WT-$gzmB^{pos}$ and WT-$gzmB^{neg}$ cells (Figure 1g). These results suggest that granzyme B may be involved in preventing IL-17 production when $CD4^+$ T cells are cultured under Th1 conditions.

$CD4^+$ T cells cultured in Th2 differentiation conditions, which contains anti-IFNγ, lack granzyme B expression (Supplemental Figure 1b); therefore, as expected, promiscuous cytokine

expression in granzyme B-deficient CD4$^+$ T cells was not observed in Th2 differentiation conditions (Supplemental Figure 1c).

In vivo activation of granzyme B-deficient CD4$^+$ T cells results in increased pathogenicity

To further understand the role of granzyme B in CD4$^+$ T cell differentiation, we adoptively transferred naïve CD4$^+$CD45RB^{hi} T cells from WT or *Gzmb*$^{-/-}$ mice into *Rag2*$^{-/-}$ recipient mice. Because it is well-established that transfer of naïve CD4$^+$ T cells into immunocompromised recipients results in chronic intestinal inflammation, [22, 23] this set up allows us to: 1) determine whether granzyme B-deficiency alters CD4$^+$ T cell pathogenicity, and 2) whether absence of granzyme B influences the cytokine profile of CD4$^+$ T cells activated *in vivo* (discussed in the next section).

In our animal colony, transfer of naïve CD4$^+$ T cells from WT mice typically results in disease symptoms by 6 weeks after transfer. However, when naïve CD4$^+$ T cells from *Gzmb*$^{-/-}$ mice were transferred into *Rag2*$^{-/-}$ mice, weight loss was evident starting at 14 days after transfer, and by day 21 these mice had lost around 20% of their original weight (Figure 2a). At this point, the experiments were terminated to comply with our institution's animal welfare regulations. In contrast, at day 21, *Rag2*$^{-/-}$ mice that received WT cells were either gaining or maintaining their weight (Figure 2a). Weight loss was accompanied by increased disease severity characterized by diarrhea, pilo-erection, and hunching (Figure 2b); increased intestinal pathology based on immune cell infiltration, loss of goblet cells, epithelial damage and hyperplasia (Figure 2c); and donor-derived CD4$^+$ T cell reconstitution (Figure 2d). To confirm that the pathogenicity observed in granzyme B-deficient CD4$^+$ T cells is an intrinsic effect, we adoptively transferred naïve CD4$^+$ T cells from littermate *Gzmb*$^{+/-}$ and *Gzmb*$^{-/-}$ mice into *Rag2*$^{-/-}$ recipient mice. Although disease

development was delayed for almost a week, *Gzmb*$^{-/-}$ mice displayed earlier disease onset and increased colon pathology compared to *Gzmb*$^{+/-}$ littermate controls (Supplemental Figure 2a), indicating that the pathogenicity observed is intrinsic to CD4^{+} T cells.

To investigate whether the recipient mice's granzyme B status is important for disease development, we adoptively transferred naïve CD4^{+} T cells from WT or *Gzmb*$^{-/-}$ donor mice into *Rag2*$^{-/-}$ *Gzmb*$^{-/-}$ recipient mice. Donor CD4^{+} T cells from WT mice did not cause early weight loss in the double knock-out recipient mice, while CD4^{+} T cells deficient in granzyme B caused similar weight loss as in *Rag2*$^{-/-}$ recipient mice (Supplemental Figure 2b and Figure 2a). Weight loss in mice receiving granzyme B-deficient CD4^{+} T cells was accompanied by increased disease severity (Supplemental Figure 2c), colon pathology (Supplemental Figure 3d), and donor-derived CD4^{+} T cell reconstitution (Supplemental Figure 3e). Therefore, the granzyme B status in the recipient mice is irrelevant for the intrinsic pathogenicity of granzyme B-deficient CD4^{+} T cells.

In summary, our data indicate that absence of granzyme B in CD4^{+} T cells activated *in vivo* results in accelerated pathogenicity and increased cell reconstitution.

Granzyme B-deficient CD4^{+} T cells present increased IL-17 production *in vivo*.

To determine whether granzyme B deficiency results in differential CD4^{+} T cell cytokine profiles *in vivo*, we adoptively transferred naïve CD4^{+}CD45RB^{hi} T cells from WT or *Gzmb*$^{-/-}$ mice into *Rag2*$^{-/-}$ recipient mice. Three weeks after transfer, donor-derived cells were recovered from the MLN and lamina propria and analyzed for IFNγ and IL-17 expression. As shown in Figure 3, IFNγ was the predominant cytokine produced by donor CD4^{+} T cells derived from WT and *Gzmb*$^{-/-}$ mice, with similar levels between WT and *Gzmb*$^{-/-}$ CD4^{+} T cells (Figure 3a and 3b). However, CD4^{+} T cells from *Gzmb*$^{-/-}$ donor mice presented significantly increased IL-17 production in

comparison to WT CD4$^+$ T cells (Figure 3a and 3b). It has been reported that pathogenesis in colitis requires the development of Th17 cells expressing IFNγ.[24] As shown in Figure 3a and 3b, the frequency of IL-17$^+$IFNγ$^+$ donor-derived CD4$^+$ T cells was similar among both groups in the MLN and lamina propria, suggesting that these cells may not be responsible for the accelerated colitis development observed. Albeit less pronounced, cytokine profiles were also similar when littermate *Gzmb*$^{+/-}$ and *Gzmb*$^{-/-}$ donor mice were used (Supplemental Figure 3).

In summary, *in vivo* activated CD4$^+$ T cells deficient in granzyme B presented increased IL-17 production. These results suggest that absence of granzyme B results in skewed *in vivo* differentiation.

Granzyme B deficient CD4$^+$ T cells present a distinct gene expression profile

Because granzyme B-deficient CD4$^+$ T cells had increased IL-17 production when activated *in vivo*, we investigated whether these cells presented a distinct gene expression profile in comparison to *in vivo* activated CD4$^+$ T cells from WT mice. For this purpose, CD4$^+$CD45RB^{hi} T cells from WT and *Gzmb*$^{-/-}$ donor mice were adoptively transferred into *Rag2*$^{-/-}$ mice. Three weeks after transfer, CD4$^+$ T cells were recovered from the MLN, their RNA extracted and gene expression profile determined by RNAseq. As shown in Figure 4a, WT and granzyme B-deficient CD4$^+$ T cells presented significantly different gene expression profiles. Examples of genes encoding transcription factors or molecules associated with gene expression upregulated in CD4$^+$ T cells derived from *Gzmb*$^{-/-}$ mice include Special AT-rich Binding protein (*Satb1*), a chromatin remodeling protein involved in T cell development and implicated in Th2 and regulatory T cell responses;[25] Krüppel-like transcription factor 13 (*Klf13*), which has been implicated in T cell survival; [26] nuclear receptor subfamily 1, group D, member 1 (*Nr1d1*), which in human T cells is

important for circadian cycles;[27] and the Th17 master transcription factor *Rorc*. We also performed gene set enrichment analysis to determine whether WT and granzyme B-deficient CD4$^+$ T cells recovered from recipient mice segregated in specific groups. As indicated in Figure 4b, GSEA indicated that these two CD4$^+$ T cell populations presented distinct differential gene expression within several GSEA groups (Figure 4b). These results indicate that granzyme B-deficient CD4$^+$ T cells, in the adoptive transfer system, follow a distinct differentiation pathway compared to WT CD4$^+$ T cells.

We validated the results generated from the RNAseq analysis by comparing the expression of selected genes in naïve CD4$^+$ T cells (Figure 4c, top), and donor-derived cells recovered 21d post-adoptive transfer (Figure 4c, bottom). Hallmark genes involved in Th17 responses, such as *Rorc* and *Il17a*, were similarly expressed in naïve CD4$^+$ T cells, regardless of the granzyme B status, but their expression was significantly increased in recovered granzyme B-deficient CD4$^+$ T cells. *Ddit4*, a gene important for optimal T cell proliferation,[28] is highly expressed in T cells from multiple sclerosis patients, and is important in Th17 differentiation.[29] *Ddit4* expression was 3-fold higher in activated CD4$^+$ T cells derived from *Gzmb*$^{-/-}$ mice in comparison to WT CD4$^+$ T cells (Figure 4c). Granzyme B-deficient CD4$^+$ T cells presented a 2-fold increase in *Il7r* expression (Figure 4c), which mediates IL-7 signaling, a well-known lymphopoietic cytokine also expressed in T cells undergoing homeostatic expansion.[30] Plexin D1, encoded by the *Plxnd1* gene, binds semaphorins[31] and is critical for directing thymocyte migration.[32] Although the role of *Plxnd1* is not well known in mature T cell biology, granzyme B-deficient CD4$^+$ T cells presented approximately a 4-fold increase in expression. Interestingly, donor CD4$^+$ T cells derived from *Gzmb*$^{-/-}$ mice presented decreased *Il10ra* expression in comparison to WT counterparts (Figure 4c).

In terms of IFNγ expression, the total count read average from the RNAseq analysis for this gene were 2940.7±1332 and 2609.3±1348.9 (P=0.66) for cells derived from WT and *Gzmb*$^{-/-}$ CD4^{+} T cells, respectively, indicating that IFNγ expression is similar among the two groups. These results confirm what we observed with intracellular staining for this cytokine (Figure 3).

Overall, these results show that in the adoptive transfer model of CD4^{+} T cell activation, granzyme B deficiency results in a distinct gene expression profile, which is characterized by genes relevant to Th17 differentiation and T cell proliferation.

Granzyme B-deficient CD4^{+} T cells possess better reconstitution capability

As indicated in Figure 2d, granzyme B-deficient CD4^{+} T cells showed greater reconstitution in the colon than WT CD4^{+} T cells when transferred into Rag-2$^{-/-}$ recipient mice. However, this observation could be due to inflammation-driven proliferation, which was more prevalent in *Rag2*$^{-/-}$ mice receiving CD4^{+} T cells from *Gzmb*$^{-/-}$ mice. To further determine the reconstitution potential of CD4^{+} T cells derived from WT and *Gzmb*$^{-/-}$ mice, we performed competitive adoptive T cell transfer experiments. For this purpose, naïve CD4^{+} T cells from WT CD45.1 and *Gzmb*$^{-/-}$ CD45.2 mice (1x10^{5} each) were adoptively co-transferred into the same *Rag2*$^{-/-}$ recipient mice. Of the total donor-derived cells obtained from the MLN, granzyme B-deficient CD4^{+} T cells presented ~60% reconstitution, whereas WT-derived cells showed ~40% reconstitution (Figure 5a). To determine whether increased cell reconstitution by granzyme B-deficient CD4^{+} T cells correlated with increased cell division, we stained the cells for Ki67 as a surrogate marker for cell division. As shown in Figure 5b, there was higher percentage of Ki67^{+} cells in granzyme-B deficient donor-derived cells. To further confirm these results, we cultured donor-derived cells without any stimulation, and measured their division potential by CFSE

dilution after 3 days. $CD4^+$ T cells from *Gzmb*$^{-/-}$ mice showed a slight increase in cell division compared to cells derived from WT mice (Figure 5c).

We also analyzed the cytokine profile of the cells derived from the competitive adoptive $CD4^+$ T cell approach. Although the IFNγ profile of co-transferred cells was similar to cells transferred alone, co-transferred WT cells presented increased IL-17 production in comparison to WT $CD4^+$ T cells transferred alone (Figure 5d, left and middle graphs). These results raise the possibility that granzyme B-deficient $CD4^+$ T cells influenced the behavior of granzyme B-competent $CD4^+$ T cells. Interestingly, co-transferred granzyme B-deficient $CD4^+$ T cells displayed a higher percentage of $IFN\gamma^+IL\text{-}17^+$ cells in comparison to WT cells (Figure 5d, right graph). *Rag2*$^{-/-}$ mice co-transferred with WT and $GzB^{-/-}$ $CD4^+$ T cells displayed similar weight loss (Figure 5e) and colon pathology (Figure 5f) to mice transferred only with $CD4^+$ T cells from *Gzmb* $^{-/-}$ mice, suggesting that the increased pathogenicity of the latter cells was maintained even in the presence of granzyme-competent $CD4^+$ T cells.

Granzyme B-deficient mice present normal cellularity and IFNγ /IL-17 production

Since *in vivo* activated granzyme B-deficient $CD4^+$ T cells possess differential gene expression and cytokine profiles, it is possible that these differences are also observed in naïve cells. To investigate this possibility, we enumerated the $CD4^+$ T cell cellularity of spleen, MLN, and IEL compartments from WT and *Gzmb*$^{-/-}$ mice. As indicated in Supplemental Figure 4a, frequencies and numbers of $TCR\beta^+CD4^+$ T cells were similar among the two groups of mice. *Ex vivo* IFNγ and IL-17 production by non-stimulated (ns) or stimulated (s) naïve $CD4^+$ T cells derived from the MLN and IEL showed no distinguishable difference between cells from WT and *Gzmb*$^{-/-}$ mice (Supplemental Figure 4b).

In summary, naïve WT and *Gzmb*$^{-/-}$ animals appear to have similar CD4^{+} T cell cellularity and basal IFNγ and IL-17 production in peripheral lymphoid organs and the intestines.

Granzyme B deficiency results in increased disease severity during *Citrobacter rodentium* infection

As demonstrated in the previous section, naïve *Gzmb*$^{-/-}$ mice have a normal CD4^{+} T cell compartment compared to WT mice. However, because we observed that activated T cells from *Gzmb*$^{-/-}$ mice became more pathogenic and had a distinct gene expression profile in the adoptive transfer model of colitis, we investigated whether *Gzmb*$^{-/-}$ mice respond properly to antigenic stimulus. For this purpose, we infected WT and *Gzmb* $^{-/-}$ mice with the extracellular bacterium *Citrobacter rodentium*, which preferentially colonizes the colon of mice and induces an IL-17/IL-22-based immune response. After infection, WT mice maintained similar weight throughout the course of the experiment; however, starting at 9 days post-infection, *Gzmb*$^{-/-}$ mice lost weight, reaching approximately ~20% loss of the starting weight by day 12 (Figure 6a). *Gzmb*$^{-/-}$ mice also presented other signs of disease, such as diarrhea, hunched posture, and pilo-erection, which were mostly absent in WT mice (Figure 6b). Despite similar colonic bacterial burden (Figure 6c), *Gzmb*$^{-/-}$ mice developed greater pathology characterized by increased infiltration and epithelial injury than WT mice (Figure 6d). Analysis of cytokine production showed that in the spleen and LP of infected *Gzmb*$^{-/-}$ mice, there was a significant increase in CD4^{+} T cells expressing IL-17, while IFNγ production was only increased in the MLN (Figure 6e).

Because innate immune cells are important for the response against *C. rodentium*, we investigated whether the absence of granzyme B in innate immune cells was responsible for the observed increased pathology in infected *Gzmb*$^{-/-}$ mice. For this purpose, *Rag-2*$^{-/-}$ and *Rag-2*$^{-/-}$

Gzmb$^{-/-}$ mice were infected with *C. rodentium* and monitored for 14 days. Both groups of mice maintained similar weights throughout the course of the experiment (Supplemental Figure 5a), indicating that the effect caused by granzyme B-deficiency is most likely associated with adaptive immune cells. To further confirm these results, we treated *Rag-2*$^{-/-}$ and *Rag-2*$^{-/-}$*Gzmb*$^{-/-}$ mice with anti-CD40 antibodies, which induce acute intestinal inflammation in the absence of T or B cells.[33] As shown in Supplemental Figure 5b, *Rag-2*$^{-/-}$ and *Rag-2*$^{-/-}$*Gzmb*$^{-/-}$ mice presented similar weight loss throughout the course of the experiment.

Interestingly, when *Gzmb*$^{+/-}$ and *Gzmb*$^{-/-}$ littermate mice were infected with *C. rodentium*, both groups displayed similar weight curves and colon colonization (Supplemental Figure 5c and 5d). However, there was a slight trend for increased IFNγ^{+}IL-17^{+} CD4^{+} T cells in the spleen of *Gzmb*$^{-/-}$ mice (Supplemental Figure 5e).

Discussion

Granzyme B expression in CD4^{+} T cells is well-documented, and has been primarily studied in the context of granzyme B/perforin-dependent regulatory T cell suppressor activity.[34] However, as our data indicate, granzyme B expression appears to be a common feature among a significant fraction of activated CD4^{+} T cells. Interestingly, not all differentiation conditions induced granzyme B expression. For example, Th0 and Th1 cells rapidly express granzyme B starting at 1-day post activation, whereas Th17 cells do not express this enzyme at any time after activation. In the former conditions, expression of granzyme B is primarily driven by the presence of irradiated splenocytes, indicating the possibility that cell-to-cell contact is important for granzyme B expression.

Although none of the cytokines involved in Th1 differentiation induced granzyme B expression above the levels observed with the addition of irradiated splenocytes, anti-IFNγ and some cytokines present in the Th17 cocktail, such as IL-6 and TGFβ prevented the expression of this enzyme, which suggests that restriction of granzyme B expression is necessary for Th17 polarization. Studies in cytotoxic $CD8^+$ T cells have shown that activation of these cells with anti-CD3 in the presence of IL-6, but not in the presence of TGFβ, induces granzyme B expression.[35] Here we show that in $CD4^+$ T cell differentiation, IL-6 does not enhance the expression of granzyme B, indicating that $CD8^+$ and $CD4^+$ T cells possess different mechanisms for modulating granzyme B production.

Granzyme B expression may not only be limited during the initial $CD4^+$ T cell priming and differentiation. For example, TGFβ is known for its role in regulatory T cell differentiation, and some of these cells require granzyme B for their suppressor functions. However, as our results indicate, TGFβ ablates expression of this enzyme, suggesting that regulatory T cells must acquire granzyme B expression during post-priming events. Similarly, a fraction of effector $CD4^+$ T cells that migrate into the intestinal intraepithelial lymphocyte compartment acquire granzyme B expression after transcriptional reprogramming.[36]

One of the most intriguing questions is: Why do $CD4^+$ T cells express granzyme B during Th0/Th1 activation and differentiation? During *in vitro* Th0/Th1 differentiation, WT-gzmB^{pos} and WT-gzmB^{neg} cells have distinct IFNγ profiles, suggesting that these cells may represent different lineages and that the activity of granzyme B influences their outcome. This is better exemplified when analyzing granzyme B-deficient $CD4^+$ T cells, where *in vivo* and *in vitro* activation skew the cells towards an IL-17-producing phenotype, with a distinct gene expression signature. We postulate that granzyme B-deficient IL-17^+ cells represent a lineage of cells that underwent

aberrant differentiation. Therefore, expression of granzyme B during Th0/Th1 activation serves as a checkpoint for proper $CD4^+$ T cell differentiation, preventing IL-17 production and increased pathology. These observations have important significance because it has been reported that allelic variants of granzyme B correlate with autoimmune disorders,[37-39] raising the possibility that in certain $CD4^+$ T cell-mediated disorders, lack of proper granzyme B function increases the probability of improper differentiation and increased pathogenesis potential. If this idea is correct, then WT-gzmB^{pos} $CD4^+$ T cells may represent cells in which the differentiation signals have the potential to skew cells into an unwanted phenotype, and granzyme B expression in these cells ensures the correct differentiation process.

We have shown that adoptive transfer of $CD4^+$ T cells derived from non-littermate (Figure 2) and littermate (Supplemental Figure 2a) mice resulted in increased pathogenicity and IL-17 production, which argues that granzyme B deficiency has an intrinsic effect in $CD4^+$ T cells. However, the host's environment also influences the pathogenicity and IL-17 production of granzyme B-deficient $CD4^+$ T cells. For example, infection of *Gzmb*$^{-/-}$ mice with *C. rodentium* resulted in more severe disease with increased IL-17 production relative to WT mice (Figure 6); however, this effect was not observed in infected *Gzmb*$^{+/-}$ and *Gzmb*$^{-/-}$ littermate mice (Supplemental Figure 5c-5e). This observation suggests that granzyme B deficiency in $CD4^+$ T cells is necessary but not sufficient for their associated increased IL-17 production and pathogenicity. One potential factor that may be responsible for controlling the pathogenicity of granzyme B-deficient $CD4^+$ T cells may be the microbiota present in granzyme B-competent mice. We are currently investigating this interesting hypothesis.

Granzyme B activity in lymphocyte development and/or differentiation has been previously reported.[40] These authors showed that granzyme A and B are important for the

development of a subset of TCR^{neg} intestinal intraepithelial lymphocytes known for the expression of intracellular CD3γ. Development of these cells requires granzyme B to cleave and inactivate the intracellular domain of Notch1. This raises the interesting possibility that during CD4$^+$ T cell differentiation, granzyme B prevents unwanted phenotypes by disrupting signals coming from the environment, such those provided by Notch and its ligands, which are known to influence CD4$^+$ T cell differentiation.[41] Our observation that granzyme B expression was increased in the presence of irradiated splenocytes supports this hypothesis. We are currently investigating what signals derived from APC enhance granzyme B expression.

It has been reported that granzyme B-deficient CD4$^+$CD25$^-$ T cells used in murine models of graft versus host disease (GVHD) induced faster disease onset with increased lethality in comparison to their WT counterparts.[42] Although this group did not provide a mechanistic explanation for the increased pathogenicity observed, they suggested that increased proliferation and decreased cell death may be involved. According to our data, we believe that in the GVHD model, differential proliferation and survival of granzyme B-deficient CD4$^+$ T cells are the result of aberrant CD4$^+$ T cell differentiation, which allows escape of highly pathogenic clones. Further investigations in the GVHD model are needed to test this hypothesis.

In summary, granzyme B has been known for its role in cell mediated-cytotoxicity, and while many groups have reported potential extracellular roles for this enzyme,[43] here we present *in vitro* and *in vivo* evidence supporting a novel intrinsic function for granzyme B during CD4$^+$ T cell differentiation. Although many questions remain to be answered regarding how granzyme B is involved in this process, our results provide a strong foundation for a better understanding of the function of this enzyme in CD4$^+$ T cell biology.

409 **Methods**

410 *Mice*. C57BL/6J and C57BL/6J.CD45.1 mice were originally purchased from The Jackson
411 Laboratory (000664, and 002014 respectively) and have been maintained and acclimated in our
412 colony for several years. Granzyme B (*Gzmb*)$^{-/-}$ mice were kindly provided by Dr. Xuefang Cao.
413 Littermate mice were generated by crossing *Gzmb*$^{-/-}$ with WT mice; F1 males (*Gzmb*$^{+/-}$) were
414 subsequently crossed to *Gzmb*$^{-/-}$ female mice to obtain *Gzmb*$^{+/-}$ and *Gzmb*$^{-/-}$ mice. CD57BL/6J
415 *Rag2*$^{-/-}$ mice were kindly provided by Dr. Luc Van Kaer. *Rag2*$^{-/-}$*Gzmb*$^{-/-}$ were generated in our
416 colony. All mice were between 6 to 10 weeks of age at the time of experimentation. Male and
417 female mice were used for all experiments. Mice were maintained in accordance with the
418 Institutional Animal Care and Use Committee at Vanderbilt University.
419
420 *Reagents and flow cytometry*. Fluorochrome-coupled anti-mouse CD4 (GK1.5), CD8α (53-6.7),
421 CD45RB (C363.16A), granzyme B (NGZB), IFNγ (XMG1.2), IL-17a (TC11-18H10), Ki67
422 (solA15), TCRβ (H57-597) and ghost viability dyes were purchased from ThermoFisher, BD
423 Bioscences or Tonbo. Biotinylated anti-CD8α (53-1.7) and CD19 (1D3) antibodies were
424 purchased from Tonbo. The Invitrogen Vybrant CFDA SE cell tracer kit was purchased from
425 ThermoFisher Scientific. Anti-CD40 antibody was purchased from BioXcell. Surface cell staining
426 was performed following conventional techniques. For intracellular cytokine staining, cells were
427 stimulated with PMA and ionomycin in the presence of Golgi Stop (BD Biosciences) for 4hr prior
428 to staining. Extracellular markers were stained, cells were fixed briefly with 2% paraformaldehyde,
429 followed by permeabilization and intracellular staining. For intracellular cytokine and granzyme
430 B staining, the BD Cytofix/Cytoperm kit was used according to the manufacturer's instructions.
431 For intracellular Ki67 staining, the eBioscience transcription factor staining buffer set was used

according to the manufacturer's instructions. All stained samples were acquired using BD FACS Canto II, 3- or 4-Laser Fortessa, or 5-Laser LSR II flow cytometers (BD Bioscences). Data were analyzed using FlowJo software (Tree Star).

Lymphocyte isolation. Spleen and MLN lymphocytes were isolated by conventional means. IEL and LP cells were isolated by mechanical disruption as previously reported.[44] Briefly, after flushing the intestinal contents with cold HBSS and removing excess mucus, the intestines were cut into small pieces (~1 cm long) and shaken for 45 minutes at 37°C in HBSS supplemented with 5% fetal bovine serum and 2 mM EDTA. Supernatants were recovered and cells isolated using a discontinuous 40/70% Percoll (General Electric) gradient. To obtain lamina propria lymphocytes, intestinal tissue was recovered and digested with collagenase (187.5 U/ml, Sigma) and DNase I (0.6 U /ml, Sigma). Cells were isolated using a discontinuous 40/70% Percoll gradient.

In vitro *CD4 T cell activation/differentiation.* Naïve CD4 T cells were isolated from the spleens of the indicated mice by magnetic sorting using the Miltenyi or StemCell Technologies naïve $CD4^+$ T cell isolation kits according to the manufacturer's instructions. Splenocytes or MLN cells used as APC were incubated for 1hr at 37°C, non-adherent cells were removed, adherent cells were washed and resuspended in complete RPMI, and irradiated with 7 Gy (700 rads). $5x10^5$ $CD4^+$ T cells with or without $5x10^5$ irradiated APC were incubated in the presence of plate bound anti-CD3 (5μg/ml) and soluble anti-CD28 (2.5μg/ml), for the indicated times, under the following conditions: Th0 (10ng/mL IL-2), Th1 (10ng/mL IL-2, 20ng/mL IL-12, and 10μg/mL anti-IL-4) , Th17 (5ng/mL TGFβ, 20ng/mL IL-6, 10ng/mL IL-1β, 10ng/mL IL-23, 10μg/mL anti-IL-4, and 10μg/mL anti-IFNγ), and Th2 (10ng/mL IL-4, 2μg/mL anti-IFNγ, and 2μg/mL anti IL-12).

455

456 *Adoptive transfer of naïve CD4 T cells*. Splenocytes from WT or *Gzmb*$^{-/-}$ mice were depleted of
457 CD19^{+} and CD8α^{+} cells using magnetic bead sorting (Miltenyi). Enriched cells were stained with
458 antibodies directed against TCRβ, CD4 and CD45RB, and naïve CD4^{+} T cells were sorted as
459 CD4^{+}CD45RB^{hi} using a FACSAria III at the Flow Cytometry Shared Resource at VUMC. 1x10^{5}
460 cells were adoptively transferred into the indicated recipient mice. Starting weight was determined
461 prior to injection. Mice were monitored and weighed weekly. At the end time point, mice were
462 sacrificed and donor-derived cells were isolated from the indicated organs or tissues. Colon
463 histopathology was performed in a blind fashion by a GI pathologist (MBP), following established
464 parameters.[45] For competitive transfer experiments, 1x10^{5} CD4^{+}CD45RB^{hi} cells from both WT-
465 CD45.1 and *Gzmb*$^{-/-}$ CD45.2 mice were adoptively co-transferred into *Rag2*$^{-/-}$ mice and analyzed
466 as indicated above.

467

468 *Transcription profile analysis*. For gene expression analysis, TCRβ^{+}CD4^{+} T cells were purified by
469 flow cytometry from a pool of MLN cells comprised of 1 male and 1 female animal with similar
470 disease progression 21 days after adoptive transfer. RNA was isolated using the RNeasy micro kit
471 (Qiagen). cDNA library preparation and RNAseq was performed by the VANTAGE Core at
472 VUMC on an Illumina NovaSeq 6000 (2 x 150 base pair, paired-end reads). The tool Salmon[46]
473 was used for quantifying the expression of RNA transcripts. The R project software along with the
474 edgeR method[47] was used for differential expression analysis. For gene set enrichment analysis
475 (GSEA), RNAseq data was ranked according to the t-test statistic. The gene sets curated (C2), GO
476 (C5), immunological signature collection (C7) and hallmarks of cancer (H) of the Molecular

Signatures Database (MSigDB) were used for enrichment analysis. GSEA enrichment plots were generated using the GSEA software[48] from the Broad Institute with 1000 permutations.

Real time PCR. For *in vitro* analysis, RNA was extracted from MACS-enriched, differentiated $CD4^+$ T cells at day 1 and 3 of culture. For *in vivo* analysis, RNA was isolated from flow cytometry purified donor-derived $TCR\beta^+CD4^+$ T cells as described above. cDNA was synthesized using the RT2 First Strand kit (Qiagen). Real time PCR was performed using RT2 SYBR Green Mastermix (Qiagen) on an Applied BioSystems Proflex PCR cycler. All primers were purchased from Qiagen.

Citrobacter rodentium *infection*. Seven-week old female WT and *Gzmb*$^{-/-}$ or *Gzmb*$^{+/-}$ and *Gzmb*$^{-/-}$ littermate animals were infected with *C. rodentium* as previously described[49]. Briefly, mice were infected with $5x10^8$ CFU exponentially grown bacteria by oral gavage. Starting weight was determined prior to gavage. Mice were monitored and weighed daily for 14d. At the end time point, cells were isolated from the indicated organs or tissues. Cellularity was determined, intracellular cytokine staining was performed, and colon histopathology was performed in a blind fashion by a GI pathologist (MBP) as previously described.[50]

Anti-CD40 disease induction. *Rag-2*$^{-/-}$ and *Rag-2*$^{-/-}$*Gzmb*$^{-/-}$ mice were injected i.p. with 150µg/mouse of anti-CD40 (BioXcell). Mice were monitored and weighed for daily for 7 days.

References

1. Anthony DA, Andrews DM, Watt SV, Trapani JA, Smyth MJ. Functional dissection of the granzyme family: cell death and inflammation. *Immunol Rev* 2010; **235**(1)**:** 73-92.

2. Chowdhury D, Lieberman J. Death by a thousand cuts: granzyme pathways of programmed cell death. *Annu Rev Immunol* 2008; **26:** 389-420.

3. Afonina IS, Cullen SP, Martin SJ. Cytotoxic and non-cytotoxic roles of the CTL/NK protease granzyme B. *Immunol Rev* 2010; **235**(1)**:** 105-116.

4. Wensink AC, Hack CE, Bovenschen N. Granzymes regulate proinflammatory cytokine responses. *J Immunol* 2015; **194**(2)**:** 491-497.

5. Kumar AA, Delgado AG, Piazuelo MB, Van Kaer L, Olivares-Villagomez D. Innate CD8alphaalpha(+) lymphocytes enhance anti-CD40 antibody-mediated colitis in mice. *Immun Inflamm Dis* 2017; **5**(2)**:** 109-123.

6. Parkinson LG, Toro A, Zhao H, Brown K, Tebbutt SJ, Granville DJ. Granzyme B mediates both direct and indirect cleavage of extracellular matrix in skin after chronic low-dose ultraviolet light irradiation. *Aging Cell* 2015; **14**(1)**:** 67-77.

7. Chamberlain CM, Ang LS, Boivin WA, Cooper DM, Williams SJ, Zhao H *et al.* Perforin-independent extracellular granzyme B activity contributes to abdominal aortic aneurysm. *Am J Pathol* 2010; **176**(2)**:** 1038-1049.

8. Lancki DW, Hsieh CS, Fitch FW. Mechanisms of lysis by cytotoxic T lymphocyte clones. Lytic activity and gene expression in cloned antigen-specific CD4+ and CD8+ T lymphocytes. *J Immunol* 1991; **146**(9)**:** 3242-3249.

9. Ebnet K, Chluba-de Tapia J, Hurtenbach U, Kramer MD, Simon MM. In vivo primed mouse T cells selectively express T cell-specific serine proteinase-1 and the proteinase-like molecules granzyme B and C. *Int Immunol* 1991; **3**(1)**:** 9-19.

10. Sun Q, Burton RL, Pollok KE, Emanuel DJ, Lucas KG. CD4(+) Epstein-Barr virus-specific cytotoxic T-lymphocytes from human umbilical cord blood. *Cell Immunol* 1999; **195**(2)**:** 81-88.

11. Canaday DH, Wilkinson RJ, Li Q, Harding CV, Silver RF, Boom WH. CD4(+) and CD8(+) T cells kill intracellular Mycobacterium tuberculosis by a perforin and Fas/Fas ligand-independent mechanism. *J Immunol* 2001; **167**(5)**:** 2734-2742.

12. Yasukawa M, Ohminami H, Yakushijin Y, Arai J, Hasegawa A, Ishida Y *et al.* Fas-independent cytotoxicity mediated by human CD4+ CTL directed against herpes simplex virus-infected cells. *J Immunol* 1999; **162**(10)**:** 6100-6106.

13. Dorothee G, Vergnon I, Menez J, Echchakir H, Grunenwald D, Kubin M *et al.* Tumor-infiltrating CD4+ T lymphocytes express APO2 ligand (APO2L)/TRAIL upon specific stimulation with autologous lung carcinoma cells: role of IFN-alpha on APO2L/TRAIL expression and -mediated cytotoxicity. *J Immunol* 2002; **169**(2)**:** 809-817.

14. Grossman WJ, Verbsky JW, Tollefsen BL, Kemper C, Atkinson JP, Ley TJ. Differential expression of granzymes A and B in human cytotoxic lymphocyte subsets and T regulatory cells. *Blood* 2004; **104**(9)**:** 2840-2848.

15. Koonpaew S, Shen S, Flowers L, Zhang W. LAT-mediated signaling in CD4+CD25+ regulatory T cell development. *J Exp Med* 2006; **203**(1)**:** 119-129.

16. Kawamura K, Kadowaki N, Kitawaki T, Uchiyama T. Virus-stimulated plasmacytoid dendritic cells induce CD4+ cytotoxic regulatory T cells. *Blood* 2006; **107**(3)**:** 1031-1038.

17. Price JD, Schaumburg J, Sandin C, Atkinson JP, Lindahl G, Kemper C. Induction of a regulatory phenotype in human CD4+ T cells by streptococcal M protein. *J Immunol* 2005; **175**(2)**:** 677-684.

18. Gondek DC, Lu LF, Quezada SA, Sakaguchi S, Noelle RJ. Cutting edge: contact-mediated suppression by CD4+CD25+ regulatory cells involves a granzyme B-dependent, perforin-independent mechanism. *J Immunol* 2005; **174**(4)**:** 1783-1786.

19. Zhu J, Yamane H, Paul WE. Differentiation of effector CD4 T cell populations (*). *Annu Rev Immunol* 2010; **28:** 445-489.

20. Sharma V, Delgado M, Ganea D. Granzyme B, a new player in activation-induced cell death, is down-regulated by vasoactive intestinal peptide in Th2 but not Th1 effectors. *J Immunol* 2006; **176**(1)**:** 97-110.

21. Coomes SM, Kannan Y, Pelly VS, Entwistle LJ, Guidi R, Perez-Lloret J *et al.* CD4(+) Th2 cells are directly regulated by IL-10 during allergic airway inflammation. *Mucosal immunology* 2017; **10**(1)**:** 150-161.

22. Powrie F, Correa-Oliveira R, Mauze S, Coffman RL. Regulatory interactions between CD45RBhigh and CD45RBlow CD4+ T cells are important for the balance between protective and pathogenic cell-mediated immunity. *J Exp Med* 1994; **179**(2)**:** 589-600. PMC2191378.

23. Powrie F, Leach MW, Mauze S, Menon S, Caddle LB, Coffman RL. Inhibition of Th1 responses prevents inflammatory bowel disease in scid mice reconstituted with CD45RBhi CD4+ T cells. *Immunity* 1994; **1**(7)**:** 553-562.

24. Harbour SN, Maynard CL, Zindl CL, Schoeb TR, Weaver CT. Th17 cells give rise to Th1 cells that are required for the pathogenesis of colitis. *Proc Natl Acad Sci U S A* 2015; **112**(22)**:** 7061-7066.

25. Zelenka T, Spilianakis C. SATB1-mediated chromatin landscape in T cells. *Nucleus* 2020; **11**(1)**:** 117-131.

26. Zhou M, McPherson L, Feng D, Song A, Dong C, Lyu SC *et al.* Kruppel-like transcription factor 13 regulates T lymphocyte survival in vivo. *J Immunol* 2007; **178**(9)**:** 5496-5504.

27. Bollinger T, Leutz A, Leliavski A, Skrum L, Kovac J, Bonacina L *et al.* Circadian clocks in mouse and human CD4+ T cells. *PLoS One* 2011; **6**(12)**:** e29801.

28. Reuschel EL, Wang J, Shivers DK, Muthumani K, Weiner DB, Ma Z *et al.* REDD1 Is Essential for Optimal T Cell Proliferation and Survival. *PLoS One* 2015; **10**(8)**:** e0136323.

29. Zhang F, Liu G, Li D, Wei C, Hao J. DDIT4 and Associated lncDDIT4 Modulate Th17 Differentiation through the DDIT4/TSC/mTOR Pathway. *J Immunol* 2018; **200**(5)**:** 1618-1626.

30. Fry TJ, Mackall CL. The many faces of IL-7: from lymphopoiesis to peripheral T cell maintenance. *J Immunol* 2005; **174**(11)**:** 6571-6576.

31. Carvalheiro T, Rafael-Vidal C, Malvar-Fernandez B, Lopes AP, Pego-Reigosa JM, Radstake T *et al.* Semaphorin4A-Plexin D1 Axis Induces Th2 and Th17 While Represses Th1 Skewing in an Autocrine Manner. *Int J Mol Sci* 2020; **21**(18).

32. Choi YI, Duke-Cohan JS, Ahmed WB, Handley MA, Mann F, Epstein JA *et al.* PlexinD1 glycoprotein controls migration of positively selected thymocytes into the medulla. *Immunity* 2008; **29**(6)**:** 888-898.

33. Uhlig HH, McKenzie BS, Hue S, Thompson C, Joyce-Shaikh B, Stepankova R *et al.* Differential activity of IL-12 and IL-23 in mucosal and systemic innate immune pathology. *Immunity* 2006; **25**(2)**:** 309-318.

34. Cao X, Cai SF, Fehniger TA, Song J, Collins LI, Piwnica-Worms DR *et al.* Granzyme B and perforin are important for regulatory T cell-mediated suppression of tumor clearance. *Immunity* 2007; **27**(4)**:** 635-646.

35. Huber M, Heink S, Grothe H, Guralnik A, Reinhard K, Elflein K *et al.* A Th17-like developmental process leads to CD8(+) Tc17 cells with reduced cytotoxic activity. *Eur J Immunol* 2009; **39**(7)**:** 1716-1725.

36. Mucida D, Husain MM, Muroi S, van Wijk F, Shinnakasu R, Naoe Y *et al.* Transcriptional reprogramming of mature CD4(+) helper T cells generates distinct MHC class II-restricted cytotoxic T lymphocytes. *Nat Immunol* 2013; **14**(3)**:** 281-289.

37. Jin Y, Birlea SA, Fain PR, Gowan K, Riccardi SL, Holland PJ *et al.* Variant of TYR and autoimmunity susceptibility loci in generalized vitiligo. *The New England journal of medicine* 2010; **362**(18)**:** 1686-1697.

38. Li S, Yao W, Pan Q, Tang X, Zhao S, Wang W *et al.* Association analysis revealed one susceptibility locus for vitiligo with immune-related diseases in the Chinese Han population. *Immunogenetics* 2015; **67**(7)**:** 347-354.

39. Shen C, Gao J, Sheng Y, Dou J, Zhou F, Zheng X *et al.* Genetic Susceptibility to Vitiligo: GWAS Approaches for Identifying Vitiligo Susceptibility Genes and Loci. *Front Genet* 2016; **7:** 3.

40. Ettersperger J, Montcuquet N, Malamut G, Guegan N, Lopez-Lastra S, Gayraud S *et al.* Interleukin-15-Dependent T-Cell-like Innate Intraepithelial Lymphocytes Develop in the Intestine and Transform into Lymphomas in Celiac Disease. *Immunity* 2016; **45**(3)**:** 610-625.

41. Amsen D, Helbig C, Backer RA. Notch in T Cell Differentiation: All Things Considered. *Trends Immunol* 2015; **36**(12)**:** 802-814.

42. Du W, Leigh ND, Bian G, O'Neill RE, Mei L, Qiu J *et al.* Granzyme B-Mediated Activation-Induced Death of CD4+ T Cells Inhibits Murine Acute Graft-versus-Host Disease. *J Immunol* 2015; **195**(9)**:** 4514-4523.

43. Boivin WA, Cooper DM, Hiebert PR, Granville DJ. Intracellular versus extracellular granzyme B in immunity and disease: challenging the dogma. *Laboratory investigation; a journal of technical methods and pathology* 2009; **89**(11)**:** 1195-1220.

44. Nazmi A, Greer MJ, Hoek KL, Piazuelo MB, Weitkamp J, Olivares-Villagomez D. Osteopontin and iCD8alpha cells promote intestinal intraepithelial lymphocyte homeostasis. *J Immunol* 2020; **In press**.

45. Aranda R, Sydora BC, McAllister PL, Binder SW, Yang HY, Targan SR *et al.* Analysis of intestinal lymphocytes in mouse colitis mediated by transfer of CD4+, CD45RBhigh T cells to SCID recipients. *J Immunol* 1997; **158**(7)**:** 3464-3473.

46. Patro R, Duggal G, Love MI, Irizarry RA, Kingsford C. Salmon provides fast and bias-aware quantification of transcript expression. *Nature methods* 2017; **14**(4)**:** 417-419.

47. Robinson MD, McCarthy DJ, Smyth GK. edgeR: a Bioconductor package for differential expression analysis of digital gene expression data. *Bioinformatics* 2010; **26**(1)**:** 139-140.

48. Subramanian A, Tamayo P, Mootha VK, Mukherjee S, Ebert BL, Gillette MA *et al.* Gene set enrichment analysis: a knowledge-based approach for interpreting genome-wide expression profiles. *Proc Natl Acad Sci U S A* 2005; **102**(43)**:** 15545-15550.

49. Olivares-Villagomez D, Algood HM, Singh K, Parekh VV, Ryan KE, Piazuelo MB *et al.* Intestinal epithelial cells modulate CD4 T cell responses via the thymus leukemia antigen. *J Immunol* 2011; **187**(8)**:** 4051-4060.

682 50. Singh K, Gobert AP, Coburn LA, Barry DP, Allaman M, Asim M *et al.* Dietary Arginine
683 Regulates Severity of Experimental Colitis and Affects the Colonic Microbiome. *Front*
684 *Cell Infect Microbiol* 2019; **9:** 66.
685
686

687

688 **Figure legends**

689

690 **Figure 1**. Granzyme B expression during T cell differentiation. (a) Naïve $CD4^+$ T cells from WT
691 mice were cultured in the presence of plate-bound anti-CD3 and soluble anti-CD28 under the
692 indicated differentiation conditions, and in the absence of irradiated splenocytes. At day 1 (top)
693 and 3 (bottom), cells were recovered, RNA extracted and granzyme B mRNA expression
694 determined. Naïve $CD4^+$ T cells without stimulation were used as reference. (b) Intracellular
695 granzyme B in cells cultured as in (a), but in the presence of irradiated splenocytes. Left,
696 representative dot plot (see Supplemental Figure 1a for gating strategy). Right, data summary. (c)
697 Granzyme B expression in cells cultured in Th0, Th1 and Th17 conditions in the presence of
698 irradiated splenocytes at different time points. (d) Cells cultured in Th0 conditions in the
699 presence of irradiated splenocytes and the indicated individual cytokines, harvested 5 days after
700 culture. (e) Cells cultured with IL-2, with or without irradiated splenocytes (APC). (f) and (g),
701 intracellular IFNγ and IL-17 staining of WT and *Gzmb*$^{-/-}$ $CD4^+$ T cells cultured in Th0 or Th1
702 conditions, respectively, in the presence of irradiated splenocytes. Top, intracellular IFNγ and
703 IL-17 staining of representative concatenated plots; bottom, data summary. Each dot represents
704 an individual sample. Data are representative of at least 3 independent experiments, performed in
705 triplicate. n=6. For (d), (f) and (g), *P<0.05; **P<0.01; ***P<0.001; ****P<0.001, One-way
706 ANOVA; For (e), ***P<0.001, Student's t test.

707

708 **Figure 2**. *In vivo* activated granzyme B-deficient $CD4^+$ T cells display increased pathogenicity.
709 $1x10^5$ $CD4^+CD45RB^{hi}$ T cells from WT or *Gzmb*$^{-/-}$ donor mice were adoptively transferred into
710 *Rag2*$^{-/-}$ recipient mice. (a) Mice were weighed weekly, and (b) monitored for signs of disease.
711 Twenty-one days after transfer, (c) colon pathology was scored (left, representative micrographs;
712 right, data summary), and (d) donor-cell reconstitution of the IEL compartment in the colon was
713 determined. For (a), dotted lines represent untreated *Rag2*$^{-/-}$ mice. Each dot represents an
714 individual mouse. Data are representative of at least 3 independent experiments. n=8-10.
715 **P<0.01; ***P<0.001; ****P<0.0001; Student's t-test.

716

717 **Figure 3**. Granzyme B-deficient $CD4^+$ T cells display skewed IL-17 differentiation *in vivo*.
718 $1x10^5$ $CD4^+CD45RB^{hi}$ T cells from WT or *Gzmb*$^{-/-}$ donor mice were adoptively transferred into

719 *Rag2*$^{-/-}$ recipient mice. Three weeks after transfer, donor-derived cells were recovered from (a)
720 MLN, and (b) lamina propria, and their IFNγ/IL-17 profile was determined by intracellular
721 staining. Dot plots indicate a representative sample. Live, TCRβ^{+}CD4^{+} cells are displayed.
722 Graphs represent the summary. Each dot indicates an individual mouse. For MLN, n=11-13; for
723 lamina propria, n=7-11. Data are representative of at least 3 independent experiments. **P<0.01;
724 ****P<0.001. Student's t-Test.
725
726 **Figure 4**. Granzyme B-deficient CD4^{+} T cells activated *in vivo* display a distinct gene expression
727 profile. 1x10^{5} CD4^{+}CD45RB^{hi} T cells from WT or *Gzmb*$^{-/-}$ donor mice were adoptively
728 transferred into *Rag2*$^{-/-}$ recipient mice. Three weeks after transfer, donor-derived cells were
729 recovered from the MLN, sorted for live TCRβ^{+}CD4^{+}, their RNA isolated and sequenced. (a)
730 Representative heat map. (b) Representative gene set enrichment analysis. The green line on the
731 plots indicate the enrichment score; the black lines show where the genes related to the pathway
732 are located in the ranking; the legend at the bottom indicates whether the expression of the genes
733 correlate more with CD4^{+} T cells derived from WT or *Gzmb*$^{-/-}$ mice. (c) Real-time PCR
734 validation of selected genes. For day 0, n=2; for day 21, n=3-6. *P<0.05; **P<0.01. Student's t-
735 Test.
736
737 **Figure 5**. Granzyme B-deficient CD4^{+} T cells present greater *in vivo* reconstitution.
738 1x10^{5} CD4^{+}CD45RB^{hi} T cells from WT (CD45.1) and *Gzmb*$^{-/-}$ (CD45.2) donor mice were co-
739 transferred into the same *Rag2*$^{-/-}$ recipient mice. As controls, cells from the same donors were
740 independently transferred into *Rag2*$^{-/-}$ recipient mice. Three weeks after transfer, (a) MLN
741 reconstitution (right, representative dot plot displaying live, TCRβ^{+}CD4^{+} cells; left, summary),
742 and (b) Ki67 staining were determined. (c) *In vitro* proliferation potential measured by CFSE
743 dilution. Histograms indicate representative samples. Gray, WT; Red, *Gzmb*$^{-/-}$. The gates indicate
744 CFSE-negative cells; graph represents summary. (d) IFNγ/IL-17 production was determined
745 from cells as in (a); graphs represent single IFNγ^{+} or IL-17^{+} (left and middle, respectively), and
746 IFNγ^{+}IL-17^{+} cells (right). (e) *Rag2*$^{-/-}$ mice that received CD4^{+} T cells from both WT/*Gzmb*$^{-/-}$ or
747 only *Gzmb*$^{-/-}$ mice were weighed weekly. (f) Colon pathology was determined 3 weeks post
748 transfer. For (a) n=11; (b) n=9; (c) n=5; (d) n=4-9; (e), n=5-9. Each dot represents an individual

mouse. Data are representative of at least 2 independent experiments. *P<0.05; **P<0.01; ***P<0.001; ****P<0.0001. For (a) and (b) Student's t-Test; for (d) One-Way ANOVA.

Figure 6. Granzyme B-deficient mice present severe disease after *C. rodentium* infection. Indicated mice were orogastrically infected with *C. rodentium* ($5x10^8$ CFU/mouse) and monitored for (a) weight change, and (b) signs of disease. At 14 days post infection, colons were dissected, (c) colonization/g of colon was determined, and (d) pathology scored as indicated in the Methods section; left, representative micrographs (200X magnification); right, data summary. (e) $CD4^+$ T cell IFNγ and IL-17 expression in the indicated organs was determined. Cells were non-stimulated (ns) or stimulated (s) for 4 h with PMA/ionomycin. Each dot represents an individual mouse. For (a-d), n=7-9; for (e), 3-5. Data are representative of at least 3 independent experiments. For (a): **P<0.01; ***P<0.01; ****P<0.001; Student's t-Test. For (b): ****P<0.001; Student's t-Test. For (d) and (e): *P<0.05; **P<0.01; One-way ANOVA.

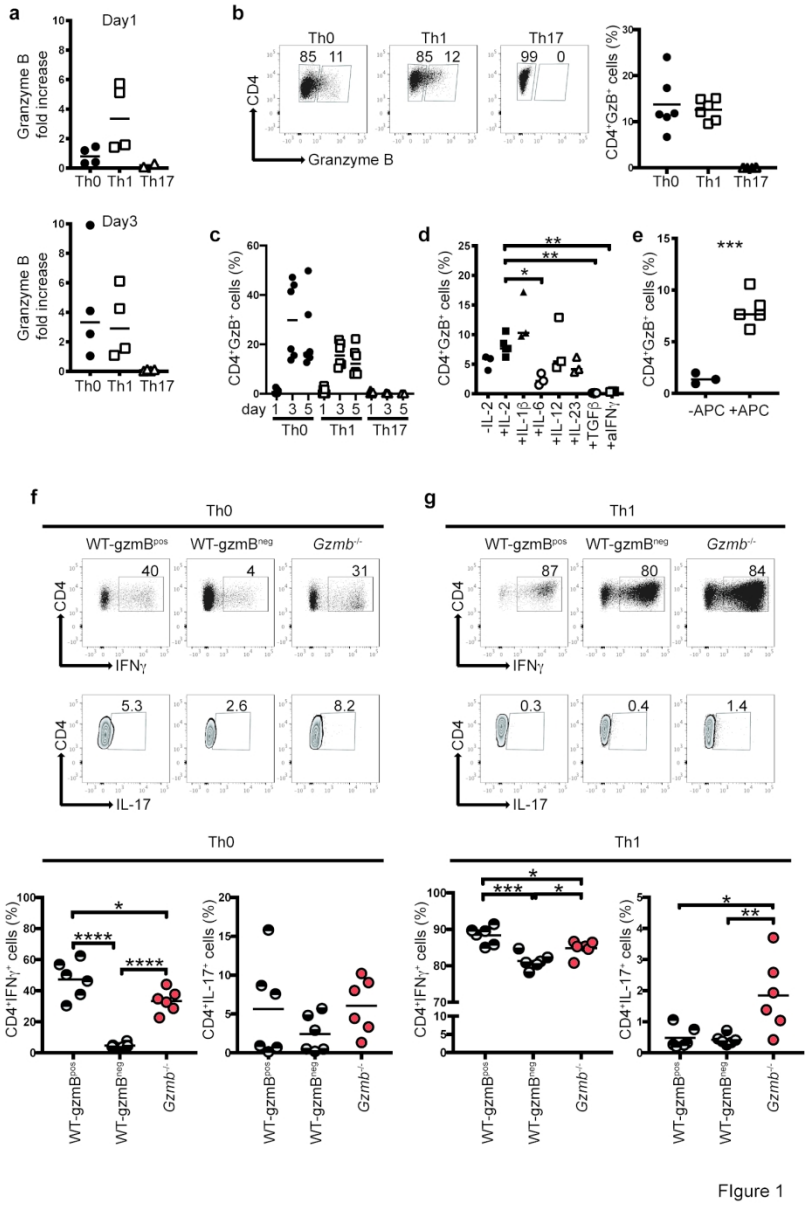

FIgure 1

Figure 1

167x246mm (240 x 240 DPI)

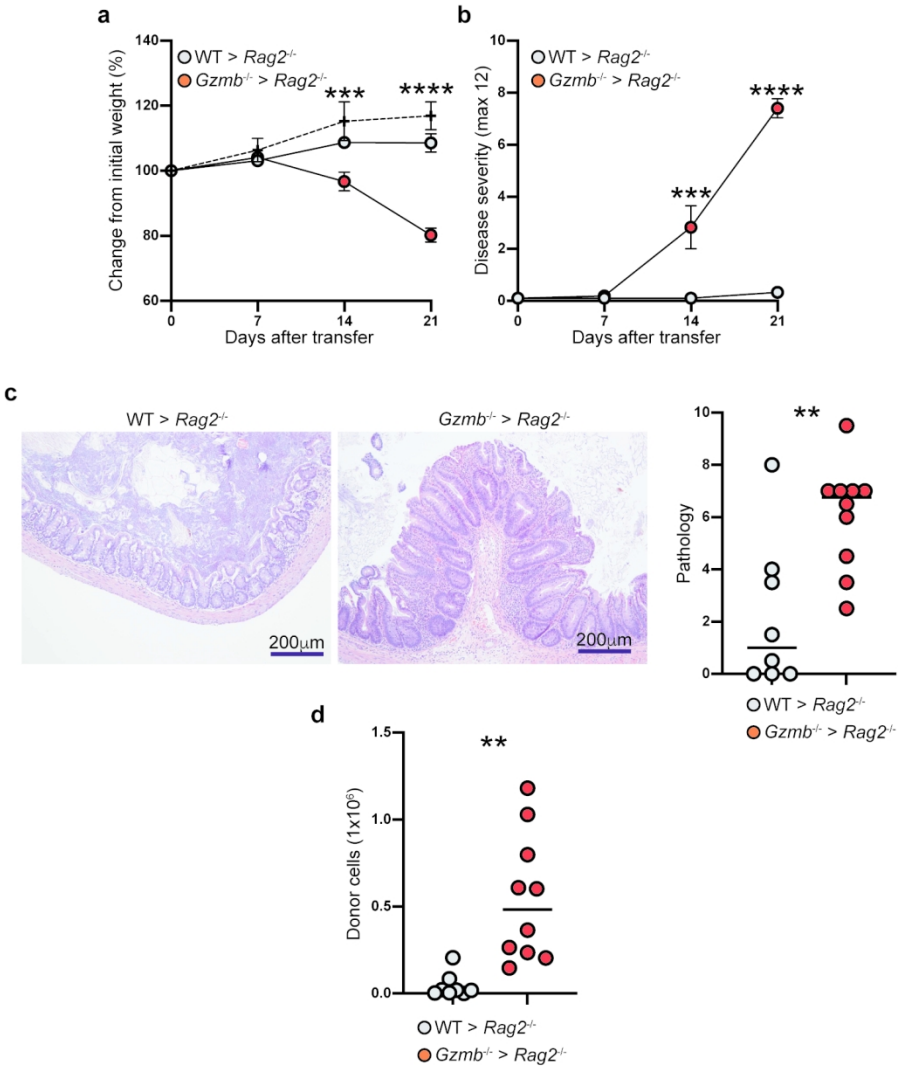

Figure 2

Figure 2

156x210mm (240 x 240 DPI)

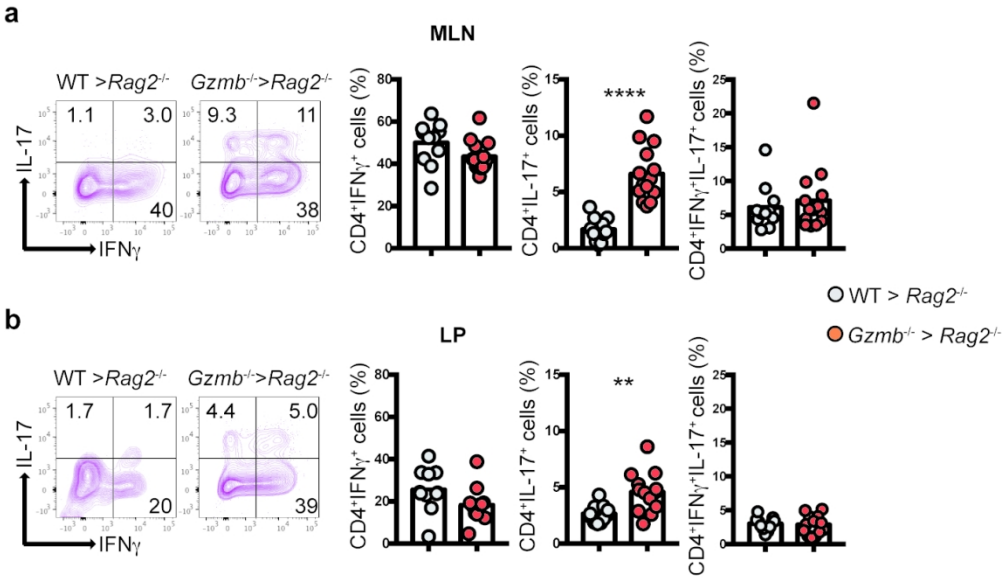

Figure 3

Figure 3

149x117mm (240 x 240 DPI)

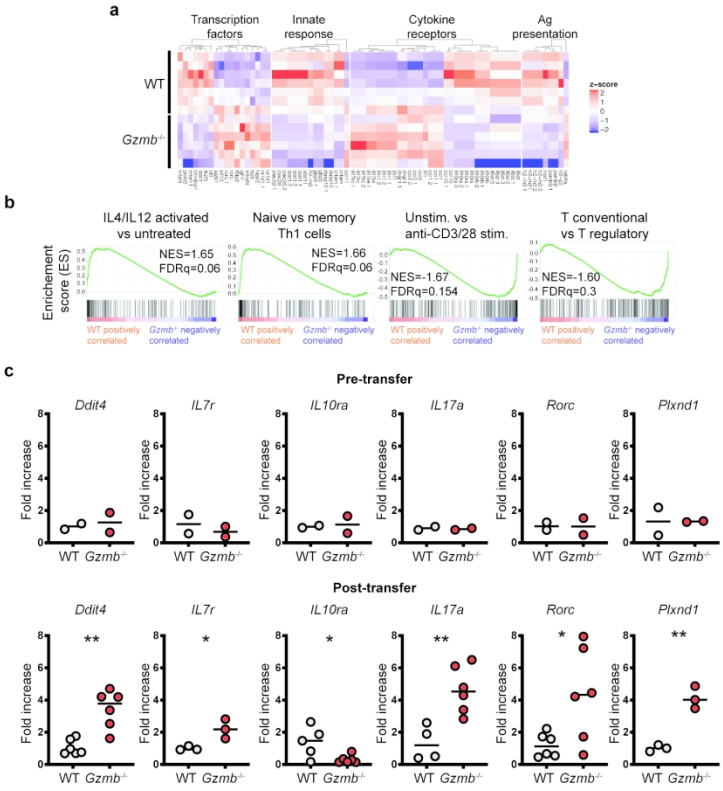

Figure 4

Figure 4

185x283mm (240 x 240 DPI)

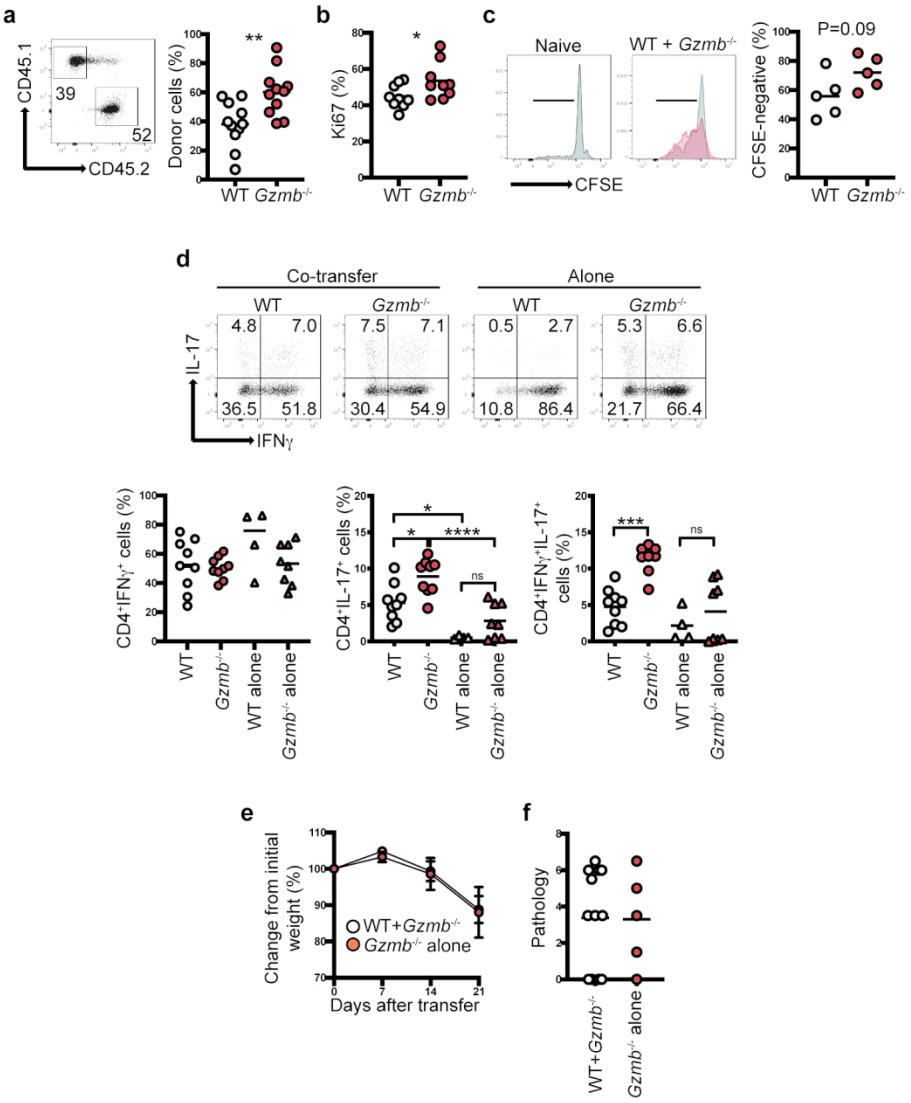

Figure 5

Figure 5

157x209mm (240 x 240 DPI)

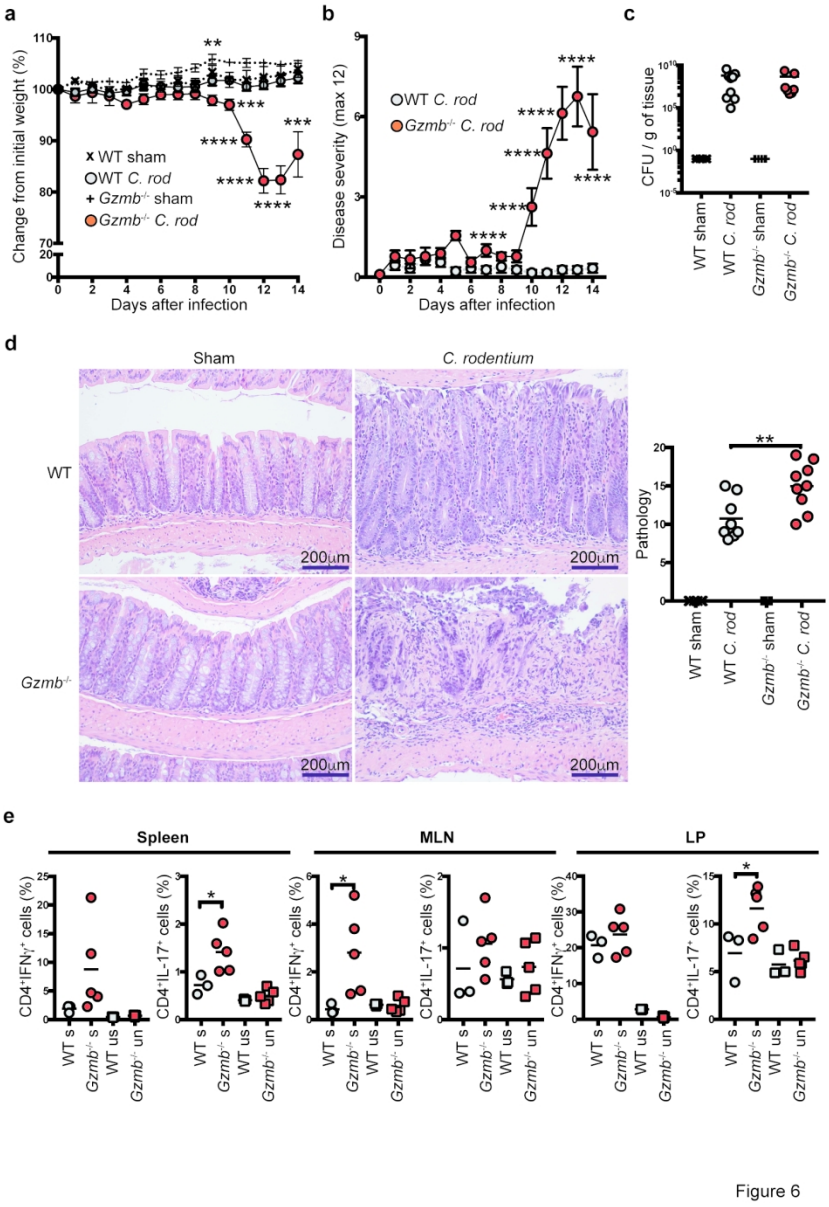

Figure 6

Figure 6

164x238mm (240 x 240 DPI)

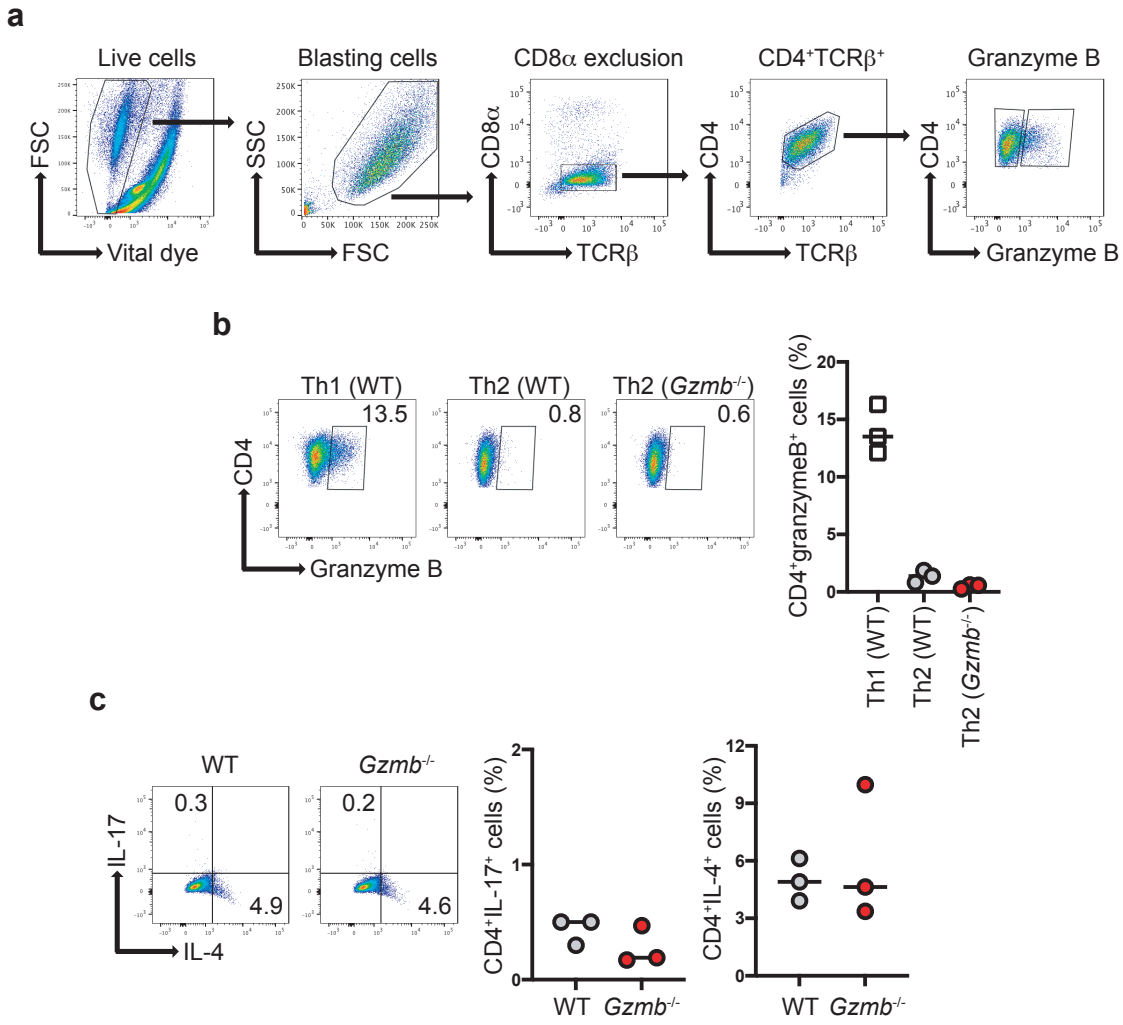

Supplemental Figure 1

Supplemental Figure 1. (a) Gating strategy for Figure 1. Plots are from representative WT $CD4^+$ T cells cultured in Th0 conditions. Cells from *Gzmb*$^{-/-}$ mice presented similar gating profiles (not shown). (b) Granzyme B expression in differentiated Th1 and Th2 cells from the indicated mice; left, representative dot plots; right, summary. n=3. (c) IL-17 and IL-4 expression in Th2 differentiated cells from the indicated mice; left, representative dot plots; right, summary. n=3.

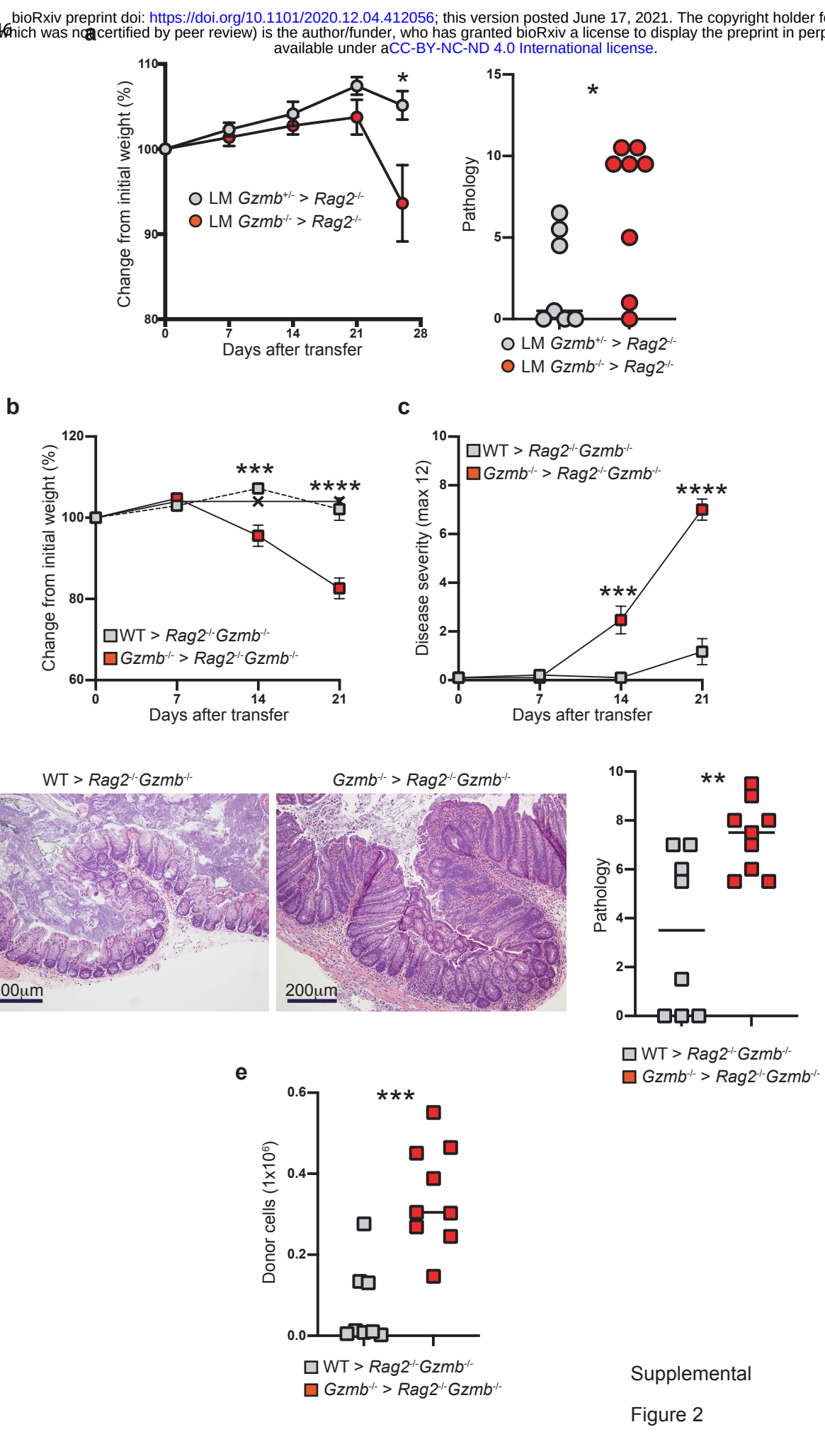

Supplemental Figure 2

Supplemental Figure 2. *In vivo* activated granzyme B-deficient $CD4^+$ T cells display increased pathogenicity. (a) $1x10^5$ $CD4^+CD45RB^{hi}$ T cells from *Gzmb*$^{+/-}$ or *Gzmb*$^{-/-}$ littermate donor mice were transferred into *Rag2*$^{-/-}$ recipient mice and their weights monitored weekly (left), and colon pathology scored (right). (b-e) $1x10^5$ $CD4^+CD45RB^{hi}$ T cells from WT or *Gzmb*$^{-/-}$ donor mice were adoptively transferred into *Rag2*$^{-/-}$*Gzmb*$^{-/-}$ recipient mice; (b) mice were weighed weekly, and (c) monitored for signs of disease. Twenty-one days after transfer, (d) colon pathology was scored (left, representative micrographs; right, data summary), and (e) donor-cell reconstitution of the IEL compartment in the colon was determined. For (a), dotted lines represent untreated *Rag2*$^{-/-}$*Gzmb*$^{-/-}$ mice. Each dot represents an individual mouse. Data are representative of at least 3 independent experiments. n=8-9. *P<0.05; **P<0.01; ***P<0.001; ****P<0.0001; Student's t-test.

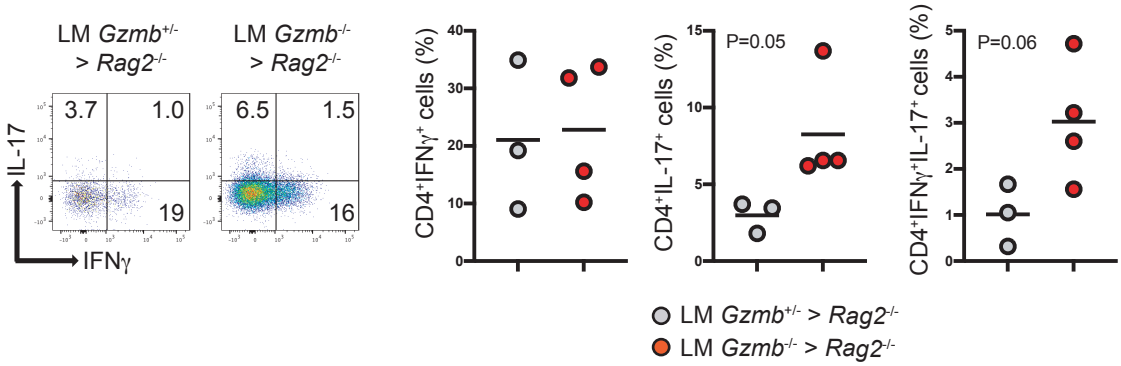

Supplemental

Figure 3

Supplemental Figure 3. Granzyme B-deficient $CD4^+$ T cells present skewed IL-17 differentiation *in vivo*. $1x10^5$ $CD4^+CD45RB^{hi}$ T cells from littermate *Gzmb*$^{+/-}$ or *Gzmb*$^{-/-}$ donor mice were adoptively transferred into *Rag2*$^{-/-}$ recipient mice. Three weeks after transfer, donor-derived cells were recovered from MLN and their IFNγ/IL-17 profile was determined by intracellular staining. Dot plots indicate a representative sample. Live, $TCR\beta^+CD4^+$ cells are displayed. Graphs represent the summary. n=3. Each dot indicates an individual mouse. Student's t-Test.

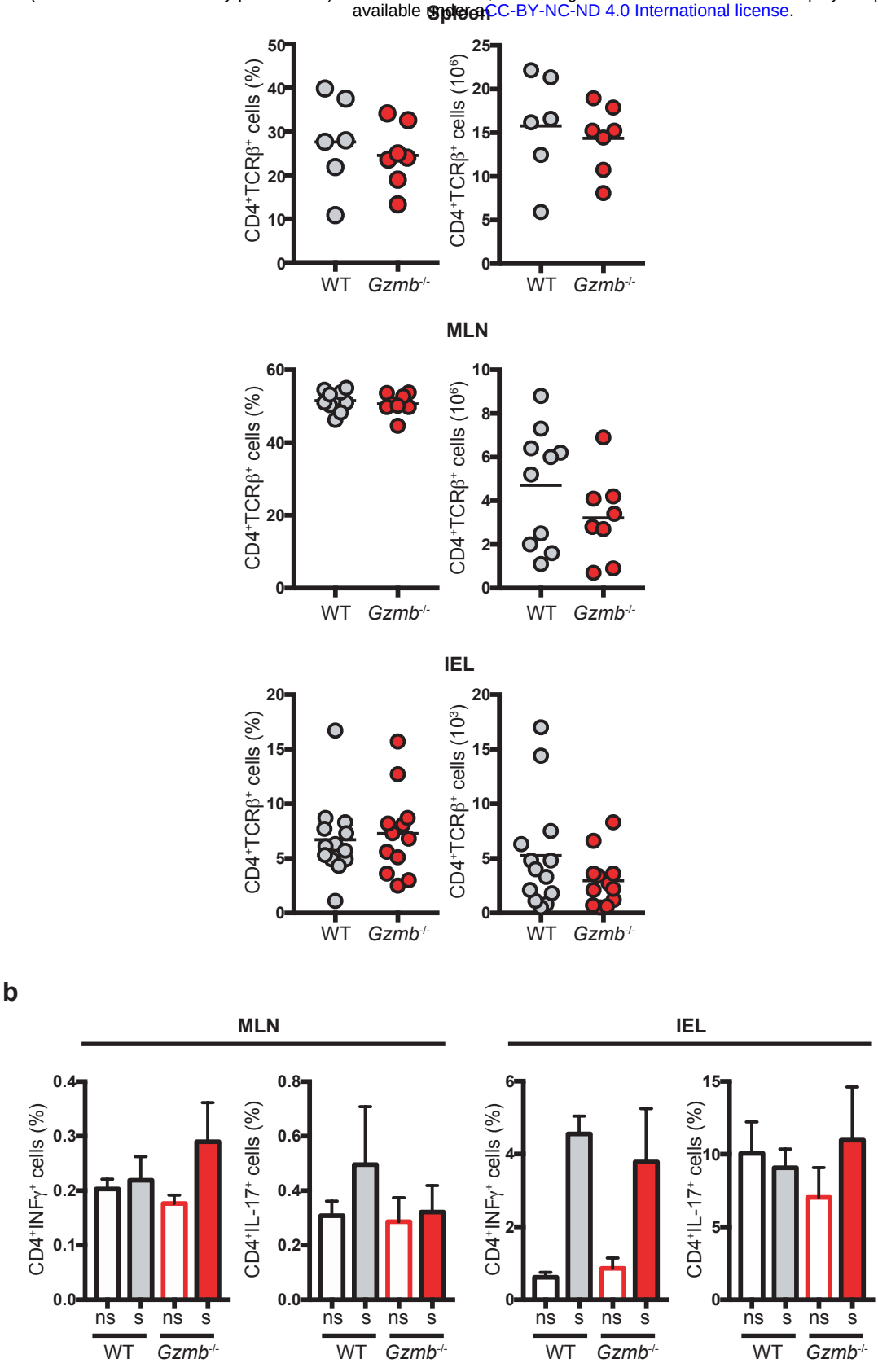

Supplemental Figure 4

Supplemental Figure 4. Naïve granzyme B-deficient mice display a normal $CD4^+$ T cell compartment. (a) $CD4^+$ T cell frequencies and cellularity from spleen, MLN, and IEL compartment were determined by flow cytometry. (b) *Ex vivo* single cytokine positive $CD4^+$ T cells derived from naïve WT and *Gzmb*$^{-/-}$ mice. Cells were non-stimulated (ns) or stimulated (s) for 4 h with PMA/ionomycin. Each dot represents an individual mouse. For (a), spleen and MLN, n=6-10; for IEL, n=12-13. For (b), n=6.

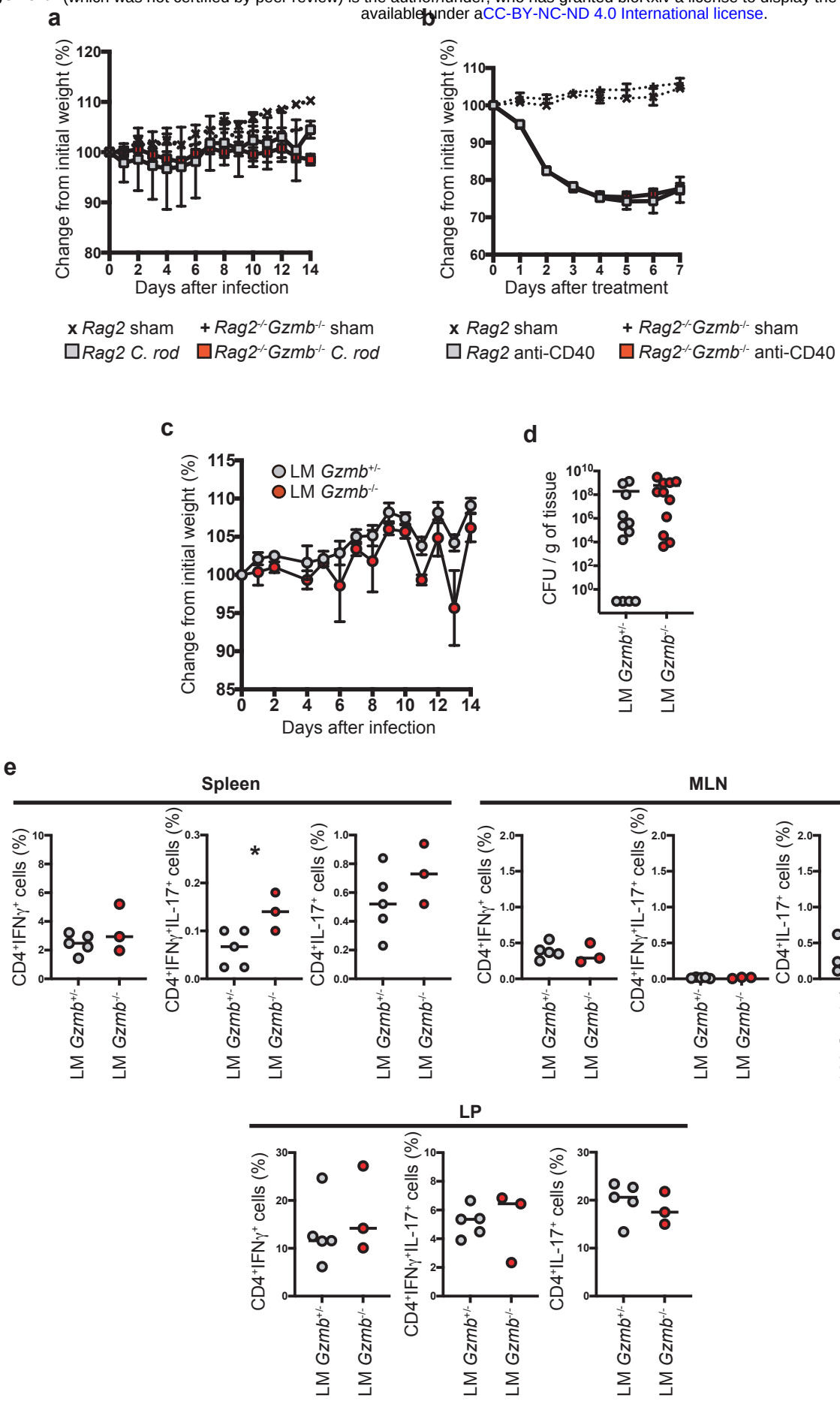

Supplemental Fig. 5

Supplemental Figure 5. (a) Absence of adaptive immune cells rescues granzyme B-deficient mice from severe disease. The indicated mice were orogastrically infected with *C. rodentium* ($5x10^8$ CFU/mouse) and monitored for weight change for 14 days. Data are representative of at least 2 independent experiments. n=3-4 for sham groups. n=5-7 for infected mice. (b) Granzyme B deficiency does not alter disease progression in the anti-CD40 model of colitis. The indicated mice were treated i.p. with 150 μg/mouse and weighed daily. Data are representative of at least 3 independent experiments. n=2 for sham groups. n=14 for treated group. (c-e) Littermate $Gzmb^{+/-}$ and $Gzmb^{-/-}$ mice were infected with *C. rodentium* ($5x10^8$ CF/mouse). (c) Animals were monitored daily for weight change. At 14 days post infection, (d) colon colonization and (e) IFNγ and IL-17 production were determined in the indicated organs. For (c and d), n=11-12; for (e), n=3-5. Student's t-Test. *$P<0.05$.